Relation-aware Isosurface Extraction in Multi-field Data

Suthambhara N and Vijay Natarajan, *Member, IEEE*

Abstract—We introduce a variation density function that profiles the relationship between multiple scalar fields over isosurfaces of a given scalar field. This profile serves as a valuable tool for multi-field data exploration because it provides the user with cues to identify interesting isovalues of scalar fields. Existing isosurface-based techniques for scalar data exploration like Reeb graphs, contour spectra, isosurface statistics, etc., study a scalar field in isolation. We argue that the identification of interesting isovalues in a multi-field data set should necessarily be based on the interaction between the different fields. We demonstrate the effectiveness of our approach by applying it to explore data from a wide variety of applications.

Index Terms—isosurface statistics, isocontours, variation density profile, persistence, multi-field data.

1 Introduction

The design of interactive and useful techniques for multi-field data remains a challenging problem. Scientists hope to understand the underlying phenomena by studying the relationship between several quantities measured or computed over a domain of interest. Therefore, multi-field data is ubiquitous to all scientific studies.

Naturally, the design of analysis and visualization techniques for multi-field data will benefit by studying the relationship between fields as opposed to a focused study of inherent properties of individual fields. We follow this principle to develop a relation-aware method for exploring scalar multi-field data.

Identification of important isovalues of scalar fields is a well studied problem. Current approaches focus on individual scalar fields and study geometric properties of the isosurface like surface area or enclosed volume, or study the topological properties abstracted into a Reeb graph or contour tree. We study this problem in the context of multi-field data. Specifically, we introduce a variation density function, whose profile is a good indicator of interesting isovalues of individual scalar fields in a multi-field dataset.

There is no unique definition for the relationship between functions in the literature. The alignment of gradients is widely used within the visualization community to quantify relationship between scalar fields [1], [2], [3]. We follow this approach and use the comparison measure proposed by Edelsbrunner et al. [1] to measure the relationship between different scalar fields.

For a given scalar field f and a sub-collection A of scalar fields from the multi-field data, the variation density function measures the relationship between scalar fields in A over isosurfaces of f. Similar to Edelsbrunner et al. [1], the variation density function quantifies the relationship between multiple scalar fields by comparing their gradients. Our hypothesis is that extrema and regions of rapid changes in the profile of the variation density function are indicative of interesting features or events in the data. Experiments on data from different applications indicate that our hypothesis is indeed true for these data sets.

• *Suthambhara is with the Department of Computer Science and Automation, Indian Institute of Science, Bangalore, India 560012.*
Vijay Natarajan is with the Department of Computer Science and Automation and the Supercomputer Education and Research Centre, Indian Institute of Science, Bangalore, India 560012.
E-mail: {suthambhara,vijayn}@csa.iisc.ernet.in

1.1 Results

Our contributions include a relation-aware approach to identification of interesting isovalues of a scalar field in a multi-field data set, a successful application of this approach to explore data from diverse application domains and a demonstration of the advantages over analyzing scalar fields in isolation. Central to the data exploration process is a variation density function that measures the relationship between scalar fields in the data. We derive links between the variation density and well understood measures like topological persistence and isosurface area statistics. We also describe a simple algorithm to compute an approximate profile of the variation density function, which provably converges to the true profile with increasing sample size. Finally, we show that our approach can be used for effective exploration of both simulation and measurement data from a wide variety of application domains.

1.2 Related Work

Bajaj et al. [4] introduced the popular *contour spectrum* as a method for exploring scalar fields by studying distributions of metric properties like area, volume, and their derivatives and integrals. Early approaches to identification of interesting isovalues study the histogram of the scalar field [5], [6].

Carr et al. [7] showed that histograms suffered from many deficiencies because they were equivalent to nearest neighbor interpolant and suggest the use of isosurface statistics computed with higher quality interpolation. Scheidegger et al. [8] proposed an improved formulation of isosurface statistics

by weighting it with the inverse gradient magnitude. This essentially means that the value of the statistic reaches infinity if the gradient vanishes. We fill this minor gap in the definition of the variation density function by excluding critical values. However, this does not affect the utility of the variation density function because we include the critical values while computing the variation density profile for piecewise linear input functions. Both Carr et al. and Scheidegger et al. mention an application of isosurface statistics to identification of interesting isovalues. Isosurface statistics considers geometric properties of an isosurface to determine its importance. For multi-field data, the importance of an isovalue additionally depends on the interaction between the different fields. In this regard, our method can be considered a generalization of their work to multi-field data. Section 5 describes this generalization in detail.

Structures like contour trees [9], and more generically Reeb graphs [10], provide an abstract representation of topological changes in isosurfaces of a scalar field as we sweep the domain in the direction of increasing / decreasing scalar value. The Reeb graph has been used as an interface for flexible extraction of individual components of interesting isosurfaces [11].

All the above methods are oblivious to other scalar fields in the data and hence do not consider relationships between fields. So, these methods may not be effective in the study of multi-field data.

Gosink et al. [2] present a method that allows visualization of interaction between three scalar fields by studying the correlation between two fields over isosurfaces of the third field. Their approach allows the classification of isosurfaces into two classes, primary and secondary, but does not provide further information to allow the identification of a smaller set of interesting isovalues. They design the method to be used within the framework of Query-Driven Visualization, which benefits from user queries.

1.3 Outline

Section 2 reviews the necessary background on comparison measure, defines the variation density function, and describes its properties. Section 3 describes an algorithm to compute the variation density profile. Section 4 reports results of experiments on 2D, 3D, and time-varying multi-field data. Section 5 discusses some properties of the variation density function and an interesting variant. Section 6 concludes the paper.

2 Variation Density Function

The variation density function measures the relationship between multiple scalar fields over isosurfaces of one of the input scalar fields. The relationship is quantified by the comparison measure introduced by Edelsbrunner et al. [1].

2.1 Comparison Measure

Let $\mathbb{M}$ be a smooth compact n-dimensional Riemannian manifold. Let $F = \{f_1, f_2, \ldots, f_k\}$ be a set of $k \leq n$ smooth real-valued functions defined on $\mathbb{M}$, $f_i : \mathbb{M} \to \mathbb{R}$. The *comparison measure*, for F, over a domain $D \subseteq \mathbb{M}$, is defined as the normalized integral

$$\kappa_D(F) = \frac{1}{vol(D)} \int_{x \in D} \|df_1 \wedge df_2 \wedge \ldots \wedge df_k\|,$$

where $vol(D)$ is the volume of D and $df_1 \wedge df_2 \wedge \ldots \wedge df_k$ is the wedge product of the k derivatives. $\kappa_{\mathbb{M}}(F)$ is called the *global comparison measure*. When D shrinks to a point $x \in \mathbb{M}$, we get the *local comparison measure*, $\kappa_x(F)$, in the limit. The product, $\kappa_D(F) \cdot vol(D)$, can be used to quantify the relationship between the different functions in F. When $k = n = 2$ and $\mathbb{M}$ is smoothly embedded in $\mathbb{R}^3$ with the standard Euclidean metric, $\kappa_x(F)$ is the length of the cross product of the two gradients at x:

$$\kappa_x(\{f_1, f_2\}) = \|\nabla f_1(x) \times \nabla f_2(x)\|.$$

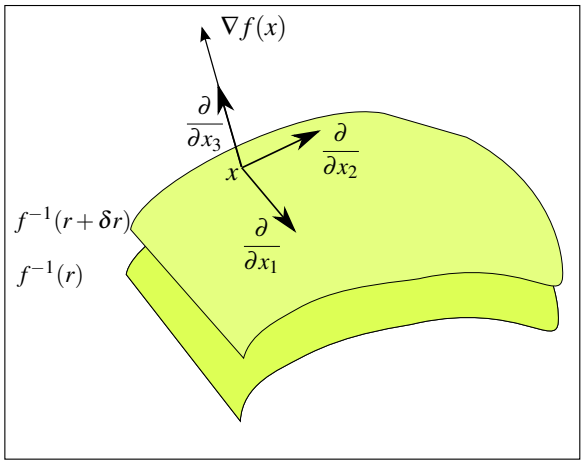

Fig. 1: Isosurfaces shown at $f^{-1}(r)$ and $f^{-1}(r+\delta r)$ when $n = 3$. It is always possible to choose a local orthonormal coordinate system such that one tangent vector $\frac{\partial}{\partial x_3}$ is aligned with the gradient of f. From the definition of gradients, it follows that $dr = \|\nabla f(x)\| dx_3$.

2.2 The Definition

For a smooth function $f : \mathbb{M} \to \mathbb{R}$, a real number c is a critical value if for some $x \in \mathbb{M}$, $\|\nabla f(x)\| = 0$ and $c = f(x)$. Let $\mathbb{P} \subseteq \mathbb{R}$ denote the set of non-critical, or *regular*, values of f.

Define a scalar function $\psi : F \times 2^F \times \mathbb{P} \to \mathbb{R}$ as

$$\psi(f, A, r) = \int_{x \in f^{-1}(r)} \frac{\kappa_x(A)}{\|\nabla f(x)\|} dS_x,$$

where dS_x is the $n-1$ dimensional isosurface area element. We assume that all the functions in F have a finite number of critical values. Given a regular value r, we can therefore choose an interval $I : [r, r+\delta r]$ that contains no critical values. We claim that

$$\int_I \psi(f, A, r) dr = \int_{x \in f^{-1}(I)} \kappa_x(A) dV_x = \kappa_{f^{-1}(I)}(A) \cdot vol(f^{-1}(I)). \quad (1)$$

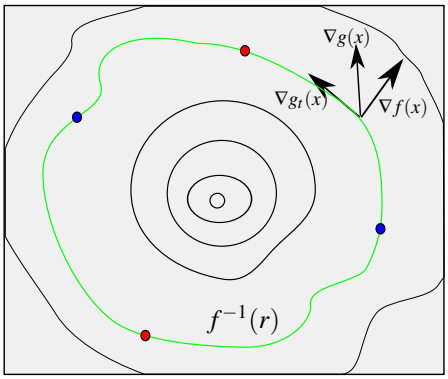

Fig. 2: Isocontours of f when $n = 2$ and $F = \{f, g\}$. The isocontour $f^{-1}(r)$ shown in green, has critical points of the restricted function g_*, at the points shown in red (maxima) and blue (minima). The ψ function is the sum of persistence values of the critical points. It also captures the total variation of g_* on the isocontour.

So, $\psi(f, A, r)$ can be considered as the density of the variation between functions in the set A. Hence, we call ψ the *variation density function*. We now prove (1) from first principles.

Consider a local coordinate system $(x_1, x_2, \ldots, x_n)$ at x such that the unit tangent vectors $(\frac{\partial}{\partial x_1}, \ldots, \frac{\partial}{\partial x_n})$ form an orthonormal basis. The volume element dV_x equals $dx = dx_1 dx_2 \ldots dx_n$. Assume, without loss of generality, that the first $n-1$ basis vectors lie on the tangent plane of $f^{-1}(r)$ at x and the last tangent vector is aligned with $\nabla f(x)$ (see Figure 1). We transform the coordinate system at x to $(x_1, x_2, \ldots, x_{n-1}, f(x))$. The volume element in the new coordinate system is obtained by multiplying with the Jacobian determinant, which is equal to the length of the gradient $\|\nabla f(x)\|$. Therefore

$$dV_x = \frac{dx_1 dx_2 \ldots dx_{n-1} dr}{\|\nabla f(x)\|}.$$

Now,

$$\begin{aligned} \int_I \psi(f, A, r) dr &= \int_I \int_{x \in f^{-1}(r)} \frac{\kappa_x(A)}{\|\nabla f(x)\|} dS_x dr \\ &= \int_I \int_{x \in f^{-1}(r)} \frac{\kappa_x(A)}{\|\nabla f(x)\|} dx_1 dx_2 \ldots dx_{n-1} dr. \end{aligned}$$

Rewriting the double integral as a single integral over $f^{-1}(I)$ and using the above expression for dV_x, we get the desired equality in (1).

2.3 Variation Density and Total Variation

In this section, we motivate the use of variation density by showing that it captures the total "variation" of a function restricted to an isosurface of the other. Specifically, we show that, for the special case of smooth functions f and g defined on a 2-manifold, the variation density is equal to the difference between the sum of values at maxima and minima of g restricted to an isocontour $f^{-1}(r)$. However, it is not clear how to extend this result to the case of multiple functions defined on a higher dimensional manifold.

Let r be a regular value of f. The isocontour $f^{-1}(r)$ is a smooth curve embedded in $\mathbb{M}$. So, we have

$$\begin{aligned} \psi(f, \{f, g\}, r) &= \int_{x \in f^{-1}(r)} \frac{\|\nabla f(x) \times \nabla g(x)\|}{\|\nabla f(x)\|} dl_x \\ &= \int_{x \in f^{-1}(r)} \|\nabla g_t(x)\| dl_x, \end{aligned} \tag{2}$$

where $\nabla g_t(x)$ is the component of $\nabla g(x)$ along the tangent to $f^{-1}(r)$ at x, and dl_x is the length element of $f^{-1}(r)$ at x (see Figure 2). Let g_* be the function obtained by restricting the domain of g to $f^{-1}(r)$. The derivative of g_* vanishes at a critical point. Critical points are either maxima or minima assuming the second derivative of g_* does not vanish at such points. Applying the fundamental theorem of calculus to each region of $f^{-1}(r)$ where g_* is monotone, we rewrite the integral of $\|\nabla g_t(x)\|$ over the isocontour $f^{-1}(r)$ as the difference between the sum of function values at maxima and minima of g_*. In other words, if C is the set of critical points of g_*, then

$$\int_{x \in f^{-1}(r)} \|\nabla g_t(x)\| dl_x = 2 \sum_{v \in C} sign(v) g_*(v), \tag{3}$$

where $sign(v)$ is either $+1$ or -1 depending on whether v is a maximum or minimum, respectively. Thus, ψ is equal to the total variation of g_* over the isocontour $f^{-1}(r)$.

The *sub-level set* of a real value s is the union of pre-images of all real values less than or equal to s. Consider the sub-level sets of g_* as we sweep $f^{-1}(r)$ in the direction of increasing value of g_*. New components are created at local minima of g_*. Components of the sub-level set merge at all maxima except for the global maximum where the sub-level set is equal to $f^{-1}(r)$. We represent each sub-level set component by its oldest minimum. When a merge happens at a maximum, we pair the maximum with the younger of the two minima representing the two merging components. The global maximum is paired with the global minimum. The *persistence* of a critical point is equal to the absolute difference in function values between the critical point and its pair. Persistence of a critical point pair represents the lifetime of a feature, *i.e.*, the time between the creation and destruction of a component in $f^{-1}(r)$ during the sweep process. Long-living components that have higher persistence values are considered to be more important.

In recent years, the notion of persistence has been used to measure, order, and simplify features [12], [13], [14], [15], [16]. This measure has been shown to be stable in the presence of noise assuming a bottleneck metric and the functions are tame [17]. From Equation (2) and Equation (3), we know that

$$\psi(f, \{f, g\}, r) = 2 \sum_{v \in C} sign(v) g_*(v). \tag{4}$$

Since every critical point is counted twice in the above expression, $\psi(f, \{f, g\}, r)$ is equal to the sum of persistence values of all critical points of g_*. The variation density function ψ, therefore, represents the total importance of all sub-level set components of g_* in $f^{-1}(r)$. This equality also suggests that

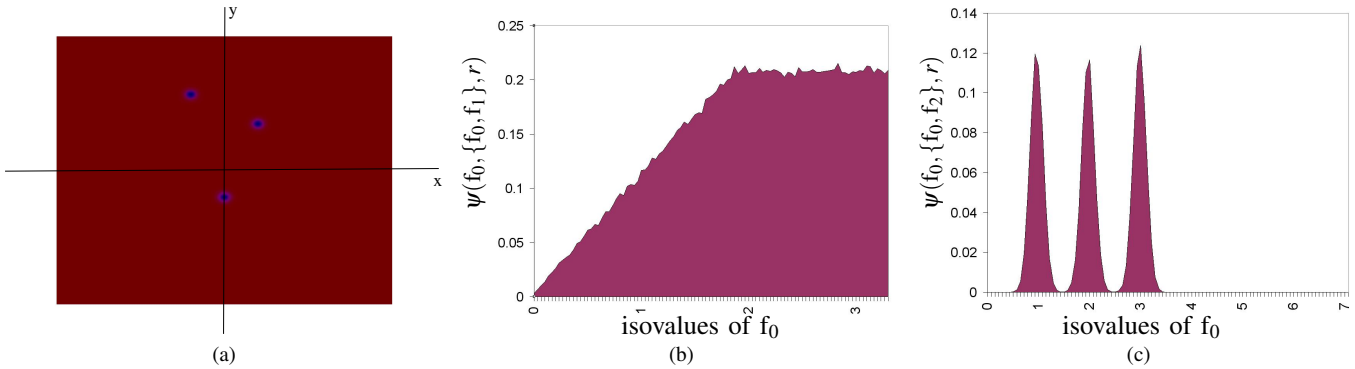

(a) (b) (c)

Fig. 3: (a) Color map of function f_2. Blue and red regions indicate low and high function values respectively. (b) The variation density profile of f_0, $\psi(f_0,\{f_0,f_1\},r)$ with $f_1(x) = \|x-2\|$. The jagged boundary of the shaded region is an artifact of using a discrete domain for computation. (c) The variation density profile of f_0, $\psi(f_0,\{f_0,f_2\},r)$, showing peaks at depressions of f_2.

we can expect the variation density function to be insensitive to small perturbations in g. This is because a small perturbation applied to the function implies a small perturbation applied to the restriction of g_*. Now, g_* and its perturbed versions are close to each oher under the L_∞ metric, which implies that the persistence values of their critical points, and hence their sum, are close to each other. Note that the function is tame because we assume that it has a finite number of critical values.

Finally, note that the integral of the expression in Equation (4) over all isovalues of f is equal to the global comparison measure as shown previously by Edelsbrunner et al [1].

2.4 Variation Density Profile

We are interested in the plot of variation density for a given scalar field f and a subset A of scalar fields. The observation that the integral of the variation density over all isovalues is the global comparison measure motivates us to study the plot of variation density against isovalues. We can consider the profile of the variation density as a plot of the contribution to the global comparison measure from the level sets of the scalar field. Given k scalar fields, only a few of the $k2^k$ possible plots are interesting. This choice of A and f is typically determined by the application. Prior knowledge of potential interaction between the scalar fields can help us make an informed choice. Each plot can provide cues that help in identifying interesting isovalues. The following examples are aimed at providing intuition behind the use of the variation density profile.

Consider the following analytic functions defined on $\mathbb{R}^2$.

$$f_0(x) = \|x\|,$$
$$f_1(x) = \|x-a\|,$$
$$f_2(x) = -(G_{a_1}(x) + G_{a_2}(x) + G_{a_3}(x)).$$

Where $x, a, a_1, a_2, a_3 \in \mathbb{R}^2$ and $G_{a_i}(x)$ is a Gaussian with a low standard deviation centered at a_i. The isocontours of f_0 and f_1 are circles centered at origin and the point a respectively. Consider an isovalue $r < \|a\|$ of f_0. The value of $\psi(f_0,\{f_0,f_1\},r)$ can be calculated from using Equation (4) to be $4r$. If $r \geq \|a\|$, we have $\psi(f_0,\{f_0,f_1\},r) = 4\|a\|$. The function ψ, therefore, increases linearly with r till the isovalue $\|a\|$ and then becomes constant.

If we consider f_0 to be elevation and f_1 to be atmospheric pressure, ψ would tell us that the variation in pressure at all points with the same elevation increases linearly till height $\|a\|$ and remains constant for higher elevations. The pressure depression at elevation $\|a\|$ is captured by a knee in the graph of ψ, see Figure 3b. Note that the corrected isocontour perimeter statistic [8] would assign the same value in the statistic graph for each isovalue of f_0. This follows from the fact that the ratio of the perimeter of an isocontour to the length of the gradient of f_0 on the isocontour is the same for all isocontours.

The function f_2 has three depressions at distances $\|a_1\|$, $\|a_2\|$ and $\|a_3\|$ from the origin. Figure 3a shows a color map of f_2 with depressions (blue regions) centered at distances $1, 2$ and 3 from the origin. The function f_2 is nearly constant at all points far away from the depressions. The variation of f_2 on an isocontour of f_0 is nearly zero if the isocontour does not pass through any of the depressions. The variation is maximum on isocontours of f_0 passing through the depressions. This results in peaks in the variation density profile (see Figure 3b). In both the examples, select isovalues of f_0 are found to be interesting only after studying the relationship between functions.

3 Computation

In this section, we describe the computation of ψ when F is a set of piecewise-linear functions and $\mathbb{M}$ is represented by an n-dimensional simplicial complex.

For $0 \leq k \leq n$, a *k-simplex* in $\mathbb{R}^n$ is the convex hull of $k+1$ affinely independent points. The interior of a simplex is the set of points in the simplex that do not lie on the boundary. Define the interior of a 0-simplex to be itself. A *simplicial complex* K is a collection of simplices such that all faces of simplices in the simplicial complex also belong to the complex and the intersection of any two simplices is empty or a face common to both. The *dimension* of K is the dimension of the simplex in K with the highest dimension. Let $\bar{f} : vertices(K) \rightarrow \mathbb{R}$ be a real valued function defined on the vertices of K. We construct a

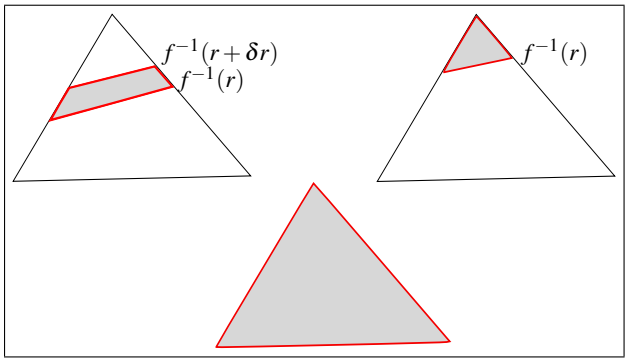

Fig. 4: Computation of ψ for a two dimensional simplicial complex. The shaded region indicates the area corresponding to a bin $[r, r+\delta r]$. This region is a small strip if the bin is contained within the range of f restricted to the triangle. The entire triangle is shaded if the bin contains the range of f restricted to the triangle or if the triangle is degenerate. If the bin and the range of f have a non-empty intersection but do not contain each other, then the shaded region contains one or two vertices of the triangle.

piecewise-linear function $f_p : K \to \mathbb{R}$ as follows. The position of any point x in the interior of a k-simplex can be written uniquely as a convex sum of the positions of vertices of the simplex, i.e, $x = \sum_1^{k+1} \gamma_i v_i$ with $\sum_1^{k+1} \gamma_i = 1$. Define $f_p(x) = \sum_1^{k+1} \gamma_i \bar{f}(v_i)$. The function f_p is continuous, linear within each simplex, and agrees with $\bar{f}$ at the vertices of K.

The gradient of f_p is well defined in the interior of a simplex and is a constant vector because f_p is linear within the simplex. The gradient vanishes inside a simplex iff the function values at all vertices of the simplex are equal. Note that a constant gradient implies that the local comparison measure is also constant in the interior of a simplex.

For a smooth function f, we first divide the range of f into a fixed number of intervals called bins. For an interval $I = [r, r+\delta r]$, define

$$\bar{\psi}(f, A, I) = \frac{\int_{f^{-1}(I)} \kappa_x(A) dx}{|I|}, \tag{5}$$

where $|I|$ is the length of the interval I. The function $\bar{\psi}(f, A, I)$ is well defined even if I contains a critical value. Note that

$$\begin{aligned} \psi(f, A, r) &= \lim_{\delta r \to 0} \frac{\int_r^{r+\delta r} \psi(f, A, r) dr}{\delta r} \\ &= \lim_{\delta r \to 0} \frac{\int_{f^{-1}(I)} \kappa_x(A) dV_x}{\delta r} \end{aligned}$$

Therefore, in the limit, when $|I| \to 0$, $\bar{\psi}$ converges to $\psi(f, A, r)$ at a regular value r.

For a piecewise-linear function f_p, we compute the integral in Equation (5) as a summation:

$$\bar{\psi}(f_p, A, I) = \frac{1}{|I|} \sum_{\sigma \in K} \kappa_\sigma * vol(interior(\sigma) \cap f_p^{-1}(I)),$$

where κ_σ is the value of κ_x for any $x \in interior(\sigma)$ (see Figure 4). Note that for piecewise-linear functions, the local comparison measure is a piecewise-constant function. Therefore, κ_x is the same for any $x \in interior(\sigma)$. The procedure ComputePsi computes the variation density profile for a given bin width h. The procedure is easily parallelizable because the computation for each simplex is independent of other simplices. The time required for a simplex inside the outer loop depends on the range of the function restricted to it and h. The worst case complexity is therefore $O(mn)$, where m and n are the number of bins and simplices respectively.

Procedure ComputePsi (f_p, A, h)

```
Initialize ψ̄(f_p, A, I) ← 0 for all bins I
for each simplex σ ∈ K do
  R ← range of f_p restricted to σ
  for each bin I such that R ∩ I ≠ φ do
    ψ̄(f_p, A, I) ← ψ̄(f_p, A, I)
      + (κ_σ * vol(f_p^{-1}(R ∩ I) ∩ interior(σ))) / h
  end for
end for
```

4 Applications

We study a variety of data using the variation density function. Our implementation works directly on simplicial complexes. If the input domain is available as a rectilinear grid, we first subdivide it into simplices by inserting diagonals and analyze the corresponding piecewise linear function. Area and volume are computed using the QHull library.

We use a fixed number of bins (100 or 200) in all our experiments. We focus on local maxima, minima and regions of steep gradients in the profile in order to identify potentially interesting isosurfaces. In all experiments, we compare our result with the isosurfaces identified using the corrected isosurface area statistic [8].

4.1 2D Combustion

We first experiment on a 2D combustion simulation data. Hydrogen fuel at 300K is mixed with an oxidizer (21% oxygen) at 1200K. The goal of the simulation is to study the influence of turbulence on the different phases of combustion. When compressed, the fuel ignites at multiple spots because of the inhomogenity in the air-fuel ratio. Depending on the air-fuel ratio, the flame either propagates in an outward direction from the ignition spot or burns out [18], [19]. The combustion is simulated on a plane over 67 time steps. The input data comprises of three scalar fields defined on a 600 x 600 grid for 67 time steps. The value of the first field at each point indicates the progress of combustion at the point. The concentrations of oxygen (O_2) and hydrogen (H_2) are the other fields.

The concentrations of H_2 and O_2 are constant away from the front of combustion. The comparison measure is therefore zero in these regions. The variation density of oxygen or hydrogen will therefore have non-zero values only for isocontours passing through the front.

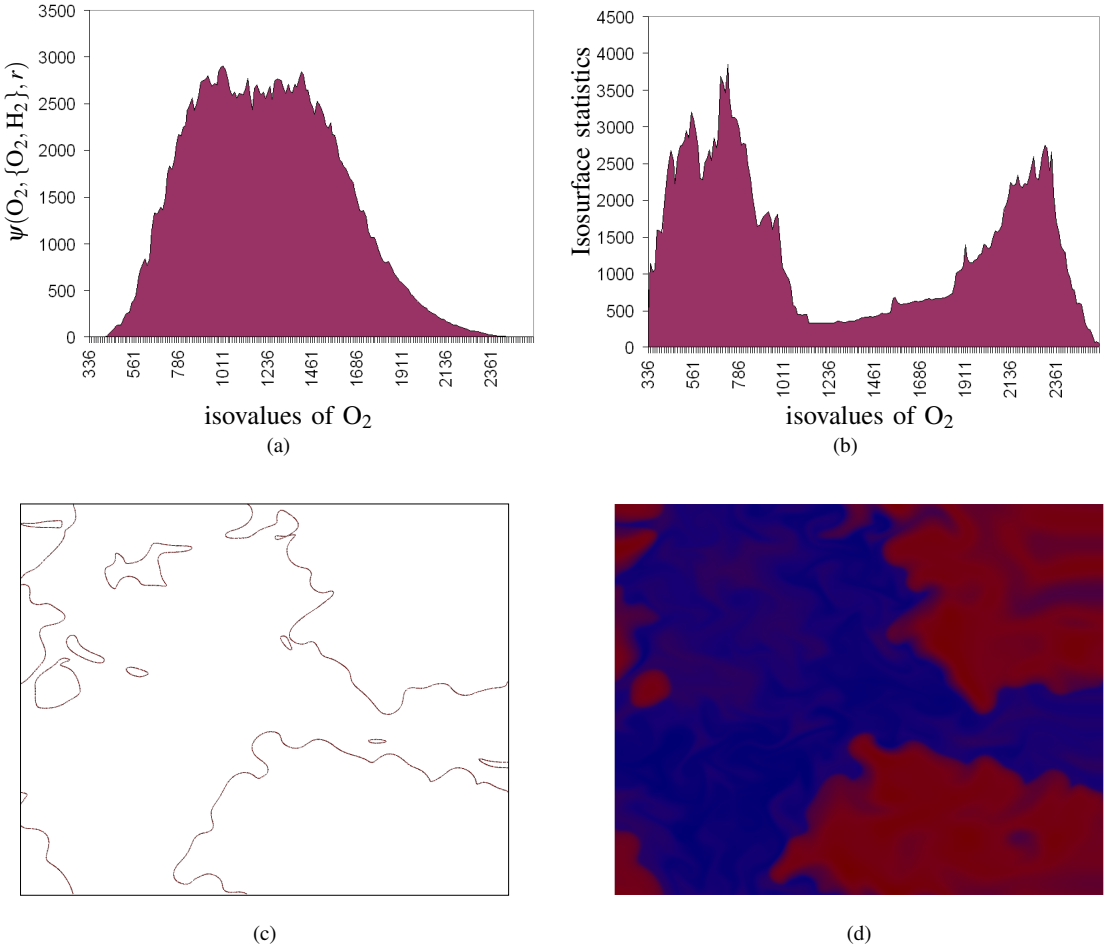

Fig. 5: Profiling isocontours of oxygen during a combustion simulation. (a) ψ computed with $f = O_2$ and $A = \{O_2, H_2\}$. (b) Isocontour statistics of O_2 do not help identify the isovalue corresponding to the front of combustion. (c) Isocontour of O_2 at 1010, the global maximum of ψ. Isocontours of oxygen in the range $(800, 1400)$ belong to the front of combustion. (d) Color map of oxygen with red and blue areas indicating high and low concentrations respectively.

For this experiment, we consider the 64^{th} time step as our input domain. The combustion is in its later stages in this time step. We profile the iscontours of oxygen considering its relationship with the fuel (hydrogen). This is accomplished by choosing $A = \{O_2, H_2\}$. The variation density profile is shown in Figure 5(a).

We observe from the profile that it increases to a maximum when the oxygen level is approximately 800 and remains high till the oxygen level is approximately 1400. We notice a gradual decline for higher isovalues. The isocontours of oxygen in this range $(800, 1400)$ belong to the front of the combustion. However, this information cannot be directly inferred from the isosurface statistic. Figure 5(c) shows the isocontour of O_2 at the value 1010, the global maximum of ψ. The front is the region where the fuel is actively burning.

The scientists who designed the simulation commented that the isocontour based segmentation of the ignition region or a burned out/extinction hole is useful in studying and understanding the nonlinear coupling that governs ignition and extinction. The shape and size of the segmented region and the correlation between the multitude of scalar fields computed within the segment play an important role in the study.

4.2 Time Varying Combustion

Next, we show the application of the variation density function to time-varying data. We consider the time varying combustion data described in the previous experiment as a three-dimensional data with time t defined as an additional scalar field. The fuel consumption rate at a point in a time step can be used to measure the progress of combustion at the point. This information is available as a scalar function `prog`.

The goal of this experiment is to identify important time phases of the combustion process. The relationship that O_2 has with time changes during the important phases of combustion. For example, on every time slice before ignition, the concentration of oxygen is nearly constant everywhere and on ignition, oxygen begins to be consumed at regions of ignition. We therefore profile the isosurfaces of time with $A = \{t, O_2\}$ (see Figure 6(a)). The profile successfully captures the ignition and the burning phases of the combustion process. The time steps $t = 27$ to $t = 35$ in the data correspond to the ignition process. This is captured as a trough in the profile. The burning

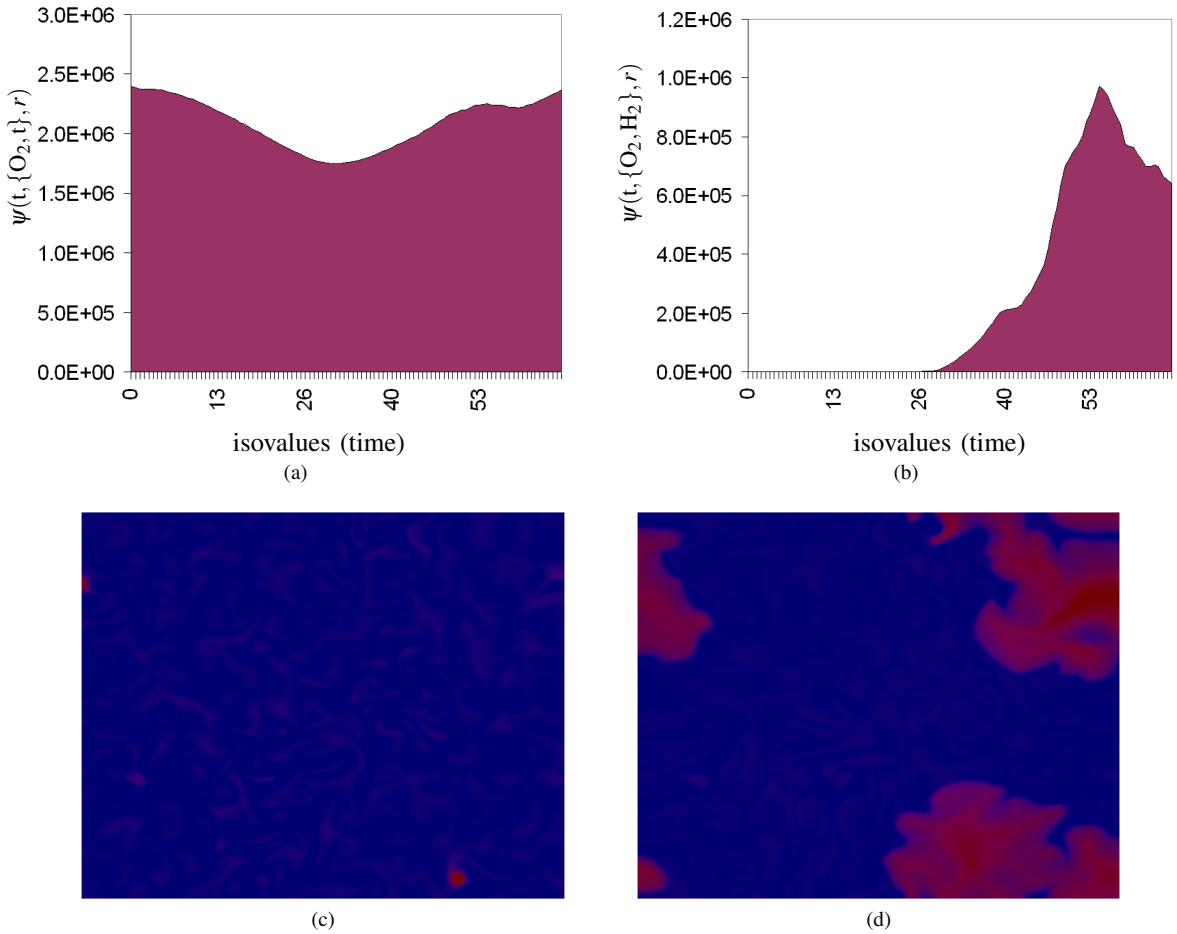

Fig. 6: Time varying combustion. (a) Variation density profile with $f = t, A = \{t, O_2\}$. (b) Profile of ψ with $f = t, A = \{H_2, O_2\}$. (c) Ignition: color-mapped image of the scalar field `prog`, which measures the completion of combustion. Red regions indicate high values and blue regions indicate low values. The distribution of `prog` in the 28^{th} time step indicates the regions where the fuel is ignited. (d) Burning: The distribution of `prog` in the 52^{nd} time step.

phase (t=50 to t=55) is also captured by a maximum in the plot. Ignition and burning are indeed considered to be the two important phases of this combustion process [19].

The interaction between O_2 and H_2 can also be considered to determine the different phases. There is no real interaction between O_2 and H_2 before ignition. We plot ψ with $A = \{O_2, H_2\}$ hoping to find more information (see Figure 6(b)). The information extracted from this profile is essentially the same compared to the profile ψ with $A = \{t, O_2\}$. The profile begins to increase from zero during the ignition phase and reaches a global maximum during the burning phase.

Isosurface statistics considers only geometric properties of a time slice and hence would not be able to detect any of the above phases. For example, the corrected area statistic would give equal importance to each isovalue and hence the plot would be a horizontal line.

The developers of the combustion simulation noted that it is desirable to identify and track transient and intermittent events like auto-ignition and extinction. They comment that our approach of studying the relationship between the air-fuel mixture over the non-local geometry of the flame front is a new idea and could help attain further insights into flame interactions.

4.3 Hurricane Isabel

Hurricane Isabel was a strong hurricane that struck the west Atlantic region in September 2003. We consider a simulation of this event [20]. The domain is a 3D rectilinear grid of size $500 \times 500 \times 100$ corresponding to a physical scale of $2139km \times 2004km \times 19.8km$. Eight scalar fields are defined over this domain. This data is defined for 48 time steps corresponding to an actual time of 48 hours. For experimental purposes, we look at only pressure (Pf) and temperature (TCf).

We study the isosurfaces of pressure at the first time step with $A = \{Pf, TCf\}$. During the initial phase of the hurricane, the eye of the storm was located in the ocean. The swirling motion around the eye corresponded to a low pressure region (-100 pascals, 20 pascals). Temperature and pressure have low correlation in this region [3]. The variation density profile shows an exponential increase for the isobars corresponding to low pressure (Figure 7(a)).

A natural question to ask is "Under what conditions do the isosurface statistics and the variation density function produce similar results?". In areas of low correlation, we observe

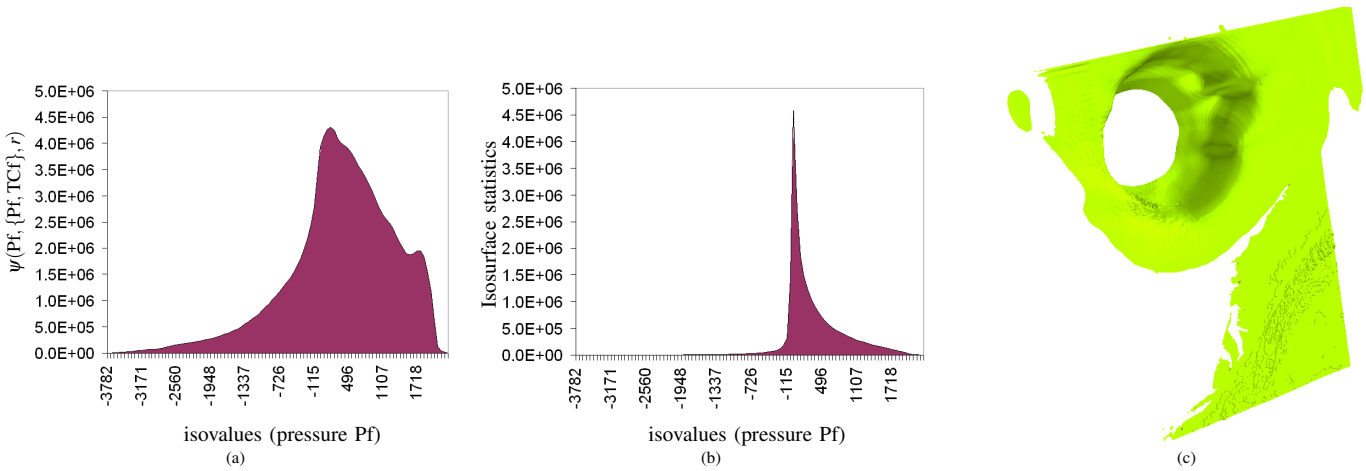

Fig. 7: Hurricane Isabel. In regions of low correlation between the fields (-100 pascals, 20 pascals) (a) the variation density function and (b) isosurface statistics behave similarly. The two values are nearly equal at isovalue 7 pascals. (c) Isobar of the hurricane at 7 pascals.

that the isosurface statistics plot (see Figure 7(b)) behaves similarly. Both exhibit an exponential increase in the region of low pressure. In fact, at approximately 7 pascals pressure, we observe that the two plots have nearly equal values. These experimental observations lead us to believe that when the input fields have a low correlation, the variation density function has no added advantage over isosurface statistics.

4.4 Universe Simulation

In the fourth experiment, we consider the simulation of ionization front instability in the universe [21]. The input domain is a $600 \times 248 \times 248$ rectilinear grid which is equivalent to a physical volume of $0.6 parsec \times 0.25 parsec \times 0.25 parsec$. The simulation is done over 200 time steps corresponding to 25.37 thousand years. The data has ten different simulated scalar fields: particle density, temperature (TCf), and eight chemical species including gaseous hydrogen (H_2), ionized hydrogen ($H+$) and ionized helium ($He+$).

The ultraviolet radiations from stars ionize hydrogen and oxygen present in space. This ionization process slows down the photons, which now proceed at a much slower pace behind a radiation wall known as the ionization front. This front separates the hot gases ($>$ 20000K), which are in an ionized state, from the ambient space at 72 K.

We study the impact of each of the chemical species on the importance of isotherms. We first study the effect of $H+$. Since hydrogen is in the ionized state, we expect to find the relevant isotherms at high temperatures. This is indeed the case (see Figure 8(b)). The profile peaks at approximately 10000K. We get similar results ionized helium ($A = \{\mathrm{TCf}, \mathrm{He}+\}$) (Figure 8(c)). The temperatures relevant for gaseous hydrogen (H_2) (Figure 8(d)) were found to be 2000-15000K, after which the plot goes to zero. This is in accord with the known fact that hydrogen is typically in the ambient state ($>$72K) or shocked state ($>$2000K). Above 15000K, hydrogen is primarily in the ionized state. Isotherms in Figures 8(e-f) correspond to isovalues identified from the variation density profile. These isovalues belong to ranges where hydrogen is in a shocked state (Figure 8e), hydrogen and helium are ionized (Figure 8f), and where there is no specific interaction between temperature and the different elements (Figure 8g). The geometry of the isotherm has no particular interpretation to the best of our knowledge.

5 Discussion

The derivation of isosurface statistics by Scheidegger et al. [8] may also be extended to develop a relation-aware statistic. In the case of three dimensional domains, isosurface statistics considers the volume enclosed by the isosurfaces $f^{-1}(r)$ and $f^{-1}(r+\delta r)$ as δr approaches zero. Normalizing this volume by the volume of the manifold, we get a probability density function that measures the probability that the scalar field assumes values between r and $r+\delta r$ as δr approaches zero. Clearly, the profile of this probability density function is the same as the isosurface statistic. However, the notion of a probability density function can be extended to two fields.

When two fields are available, we may consider the joint probability density (JPD). Rajwade et al. [22] use the JPD for two scalar fields in the context of computing mutual information and solving the image registration problem. The scalar fields are essentially grayscales of the two images that are to be registered. They show that the JPD equals

$$p(\alpha_1, \alpha_2) = \int\limits_{\{x|f(x)=\alpha_1\} \cap \{x|g(x)=\alpha_2\}} \frac{dx}{\|\nabla f(x) \times \nabla g(x)\|},$$

where f and g are the scalar fields, and α_1 and α_2 are isovalues of f and g respectively. The JPD is essentially the continuous scatterplot recently introduced by Bachthaler and Weiskopf [23]. Note that this integrand is equal to the inverse of the local comparison measure κ_x, which suggests a direct extension to multiple fields.

We also observe that the isosurface area statistic [7] and the corrected statistic [8] can be derived as special cases of

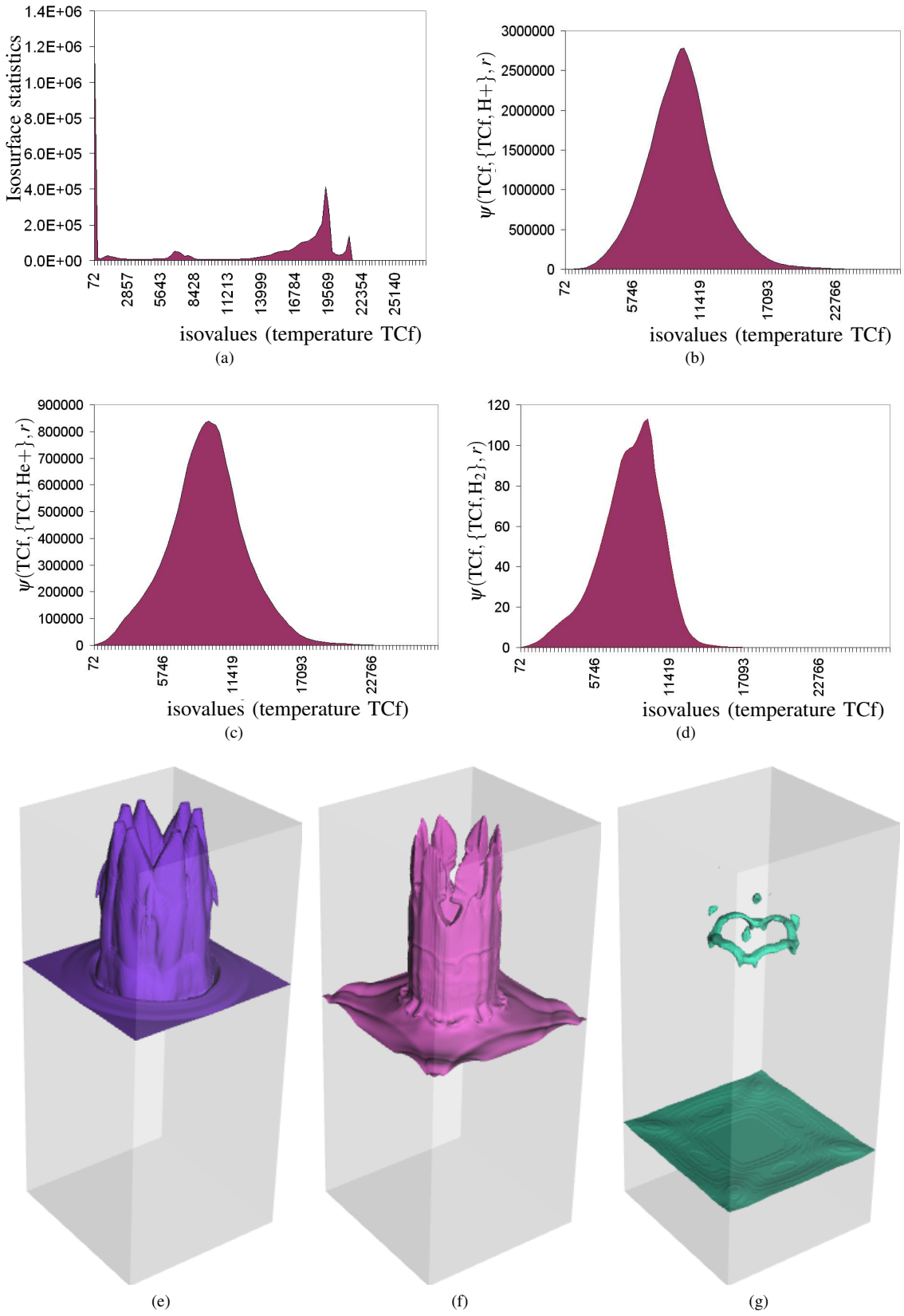

Fig. 8: Universe Simulation. (a) Isotherm statistics. (b) The profile of ψ plotted with $A = \{\text{TCf}, \text{H}+\}$. Most of the area under the curve is centered around the ionization temperature of hydrogen. Similar results are seen in (c) when $A = \{\text{TCf}, \text{He}+\}$. (d) The profile of ψ with $A = \{\text{TCf}, \text{H}_2\}$. Hydrogen in the temperature range 72-14000K is in either cool or shocked states. (e) Isotherm of universe at 3000K which lies in the range where hydrogen is in shocked state. (f) Isotherm of universe at 14500K which lies in the range where hydrogen and helium are ionized. (g) Isotherm of universe at 19500K which lies in the range where hydrogen is already ionized and there is no other significant event.

the variation density function. If the set A contains a single element f, the scalar field under consideration, then the local comparison measure $\kappa_x(\{f\}) = \|\nabla f(x)\|$. This implies that the variation density function

$$\psi(f,\{f\},r) = \int_{x \in f^{-1}(r)} dS_x,$$

which is exactly the isosurface area statistic derived by Carr et al. Now, consider the case when κ_x is a constant function, which essentially means that we have no additional information on the relationship between the scalar fields. In this case, the variation density function reduces to the corrected isosurface statistic.

The derivation in Section 2.3 indicates that the variation density function is not likely to be susceptible to noise, especially when the dimension of the domain is less than three. The derivation, however, extensively utilizes the property that regions in an isocontour can be broken into monotone paths of the restricted function g_* resulting in a closed form expression for the integrals. It is unclear if such an approach can be extended to higher dimensional domains.

6 Conclusions and Future work

We have introduced a variation density function ψ to profile isosurfaces based on relationships between different scalar fields in multi-field data. We also described an algorithm to compute the profile. The fact that ψ captures significant information that is typically not captured by isosurface statistics is evident from our experiments with several data sets from diverse real-world applications. We also conjecture that for fields with low correlation, ψ may be no better than isosurface statistics.

We list the following problems as future work:

- Characterizing the link between persistence and variation density in higher dimensions.
- Extension of our results to arbitrary number of scalar fields. Currently, the number of fields that can be compared (*i.e.* the size of the set A) is bounded by the dimension of the domain. This is primarily because the comparison measure considers the alignment of gradients of the fields to determine relationships. If the number of fields is greater than the dimension of the domain, the gradients become linearly dependent and hence the comparison measure is zero everywhere. One solution is to consider only a subset of fields at a time and then collect the different statistics together in a well defined way. In future, we would like to apply our techniques to arbitrary number of fields.
- Extending the definition of the variation density function to vector fields will be a challenging task.
- It would be interesting to see if single scalar fields can be studied more effectively using our approach. This would involve identifying suitable derived fields that can be used to profile the input scalar field.

Acknowledgments

This work was supported by the Department of Science and Technology, India under grant SR/S3/EECE/048/2007. We would like to thank Valerio Pascucci and Jackie Chen for providing the combustion data. We also thank Jackie Chen and Ajith Mascarenhas for their help with interpreting the results of our experiments on the combustion data. Hurricane Isabel data was produced by the Weather Research and Forecast (WRF) model, courtesy of NCAR and the U.S. National Science Foundation (NSF). Universe simulation data was produced by Daniel Whalen at LANL and Michael L. Norman at SDSC. We thank all reviewers for their valuable feedback, which helped improve the paper.

References

[1] H. Edelsbrunner, J. Harer, V. Natarajan, and V. Pascucci, "Local and global comparison of continuous functions," in *Proc. IEEE Conf. Visualization '04*. Washington, DC, USA: IEEE Computer Society, 2004, pp. 275–280.

[2] L. Gosink, W. Anderson, J. Bethel, and K. Joy, "Variable interactions in query-driven visualization," *IEEE Transactions on Visualization and Computer Graphics*, vol. 13, no. 6, pp. 1400–1407, 2007.

[3] N. Sauber, H. Theisel, and H.-P. Seidel, "Multifield-graphs: An approach to visualizing correlations in multifield scalar data," *IEEE Transactions on Visualization and Computer Graphics*, vol. 12, no. 5, pp. 917–924, Sept.-Oct. 2006.

[4] C. Bajaj, V. Pascucci, and D. Schikore, "The contour spectrum," in *Proc. IEEE Conf. Visualization 1997*, Oct. 1997, pp. 167–173.

[5] V. Pekar, R. Wiemker, and D. Hempel, "Fast detection of meaningful isosurfaces for volume data visualization," in *Proc. IEEE Conf. Visualization '01*. Washington, DC, USA: IEEE Computer Society, 2001, pp. 223–230.

[6] S. Tenginakai, J. Lee, and R. Machiraju, "Salient iso-surface detection with model-independent statistical signatures," in *Proc. IEEE Conf. Visualization '01*. Washington, DC, USA: IEEE Computer Society, 2001, pp. 231–238.

[7] H. Carr, B. Duffy, and B. Denby, "On histograms and isosurface statistics," *IEEE Transactions on Visualization and Computer Graphics*, vol. 12, no. 5, pp. 1259–1266, Sept.-Oct. 2006.

[8] C. E. Scheidegger, J. M. Schreiner, B. Duffy, H. Carr, and C. T. Silva, "Revisiting histograms and isosurface statistics," *IEEE Transactions on Visualization and Computer Graphics*, vol. 14, no. 6, pp. 1659–1666, 2008.

[9] H. Carr, J. Snoeyink, and U. Axen, "Computing contour trees in all dimensions," in *SODA '00: Proceedings of the eleventh annual ACM-SIAM symposium on Discrete algorithms*. Philadelphia, PA, USA: Society for Industrial and Applied Mathematics, 2000, pp. 918–926.

[10] V. Pascucci, G. Scorzelli, P.-T. Bremer, and A. Mascarenhas, "Robust on-line computation of reeb graphs: simplicity and speed," *ACM Trans. Graph.*, vol. 26, no. 3, p. 58, 2007.

[11] H. Carr, J. Snoeyink, and M. van de Panne, "Simplifying flexible isosurfaces using local geometric measures," in *Proc. IEEE Conf. Visualization '04*. Washington, DC, USA: IEEE Computer Society, 2004, pp. 497–504.

[12] P. K. Agarwal, H. Edelsbrunner, J. Harer, and Y. Wang, "Extreme elevation on a 2-manifold," *Discrete Comput. Geom.*, vol. 36, no. 4, pp. 553–572, 2006.

[13] D. Cohen-Steiner, H. Edelsbrunner, and J. Harer, "Extending persistence using Poincaré and Lefschetz duality," *Found. Comput. Math.*, vol. 9, no. 1, pp. 79–103, 2009.

[14] H. Edelsbrunner, D. Letscher, and A. Zomorodian, "Topological persistence and simplification," *Discrete Comput. Geom.*, vol. 28, no. 4, pp. 511–533, 2002.

[15] H. Edelsbrunner, D. Morozov, and V. Pascucci, "Persistence-sensitive simplification functions on 2-manifolds," in *Proceedings of the twenty-second annual symposium on Computational geometry*. New York, NY, USA: ACM, 2006, pp. 127–134.

[16] A. Gyulassy, V. Natarajan, V. Pascucci, P.-T. Bremer, and B. Hamann, "A topological approach to simplification of three-dimensional scalar functions," *IEEE Transactions on Visualization and Computer Graphics*, vol. 12, no. 4, pp. 474–484, 2006.

[17] D. Cohen-Steiner, H. Edelsbrunner, and J. Harer, "Stability of persistence diagrams," *Discrete Comput. Geom.*, vol. 37, no. 1, pp. 103–120, 2007.
[18] T. Echekki and J. H. Chen, "Direct numerical simulation of autoignition in nonhomogeneous hydrogen-air mixtures," in *Combustion and Flame*, 2003, pp. 134:169–191.
[19] W. S. Koegler, "Case study: application of feature tracking to analysis of autoignition simulation data," in *Proc. IEEE Conf. Visualization '01*. Washington, DC, USA: IEEE Computer Society, 2001, pp. 461–464.
[20] W. Wang, C. Bruyere, and B. Kuo, "Competition data set and description in 2004 IEEE Visualization design contest," http://vis.computer.org/vis2004contest/data.html.
[21] D. Whalen and M. L. Norman, "Competition data set and description in 2008 IEEE Visualization design contest," http://vis.computer.org/VisWeek2008/vis/contests.html.
[22] A. Rajwade, A. Banerjee, and A. Rangarajan, "Probability density estimation using isocontours and isosurfaces: Applications to information-theoretic image registration," *IEEE Transactions on Pattern Analysis and Machine Intelligence*, vol. 31, no. 3, pp. 475–491, March 2009.
[23] S. Bachthaler and D. Weiskopf, "Continuous scatterplots," *IEEE Transactions on Visualization and Computer Graphics*, vol. 14, no. 6, pp. 1428–1435, 2008.

Suthambhara N is a doctoral candidate at the Department of Computer Science and Automation, Indian Institute of Science, Bangalore. He holds a bachelors degree in computer science from the Vishweshwariah Technical University. His research interests include multi-field visualization and computational topology.

Vijay Natarajan is an assistant professor in the Department of Computer Science and Automation and the Supercomputer Education and Research Centre at the Indian Institute of Science, Bangalore. He received the Ph.D. degree in computer science from Duke University in 2004 and holds the B.E. degree in computer science and M.Sc. degree in mathematics from Birla Institute of Technology and Science, Pilani, India. His research interests include scientific visualization, computational geometry, computational topology, and meshing.